Title：Exploring Probability of Shallow ML Defect Impact to Defect Assurance

Authors：Kazuaki Matsui[a], Noriaki Takagi[b], Satoshi Takahashi[a], Yutaka Kodera[a], Yo Sakata[a], Shinji Akima[a]

[a]Toppan Printing Co., Ltd.

[b]EUVL Infrastructure Development Center Inc.

Publisher：Photomask Japan 2013（SPIE）

Citation：Kazuaki Matsui, Noriaki Takagi, Satoshi Takahashi, Yutaka Kodera, Yo Sakata, Shinji Akima, "Exploring Probability of Shallow ML Defect Impact to Defect Assurance," *SPIE* 8701, Photomask and Next-Generation Lithography Mask Technology XX, 87010Q (June 28, 2013); doi:10.1117/12.2031845

DOI abstract link：http://dx.doi.org/10.1117/12.2031845

We published the text from the next page

Exploring Probability of Shallow ML Defect Impact to Defect Assurance

Kazuaki Matsui[a], Noriaki Takagi[b], Satoshi Takahashi[a], Yutaka Kodera[a], Yo Sakata[a], Shinji Akima[a]

[a]Toppan Printing Co., Ltd., 7-21-33 Nobidome, Niiza, Saitama, 352-8562 Japan
[b]EUVL Infrastructure Development Center Inc., 16-1 Onogawa, Tsukuba-shi, Ibaraki 305-8569, Japan

ABSTRACT

EUV blank defect is one of the key issues the industry has to overcome to implement EUV lithography for HVM (high volume manufacturing). Several inspection techniques for EUV blank defect detection have been proposed, but the blank defect criteria for EUV mask is assumed to be very tight, thus, high sensitivity performance is required for blank inspection. However, it is important how the blank inspection tool to be assessed with appropriate test blanks with properly characterized defects. New programmed defect fabrication method has been introduced and verified that the method enables to fabricate natural-like programmed defects. In this study, it was attempted to fabricate more complex shape defects and investigated how multilayer defects are grown during multilayer deposition. Then, printability simulation was conducted for 3 different defect transition models, and critical multilayer defect shapes and sizes were discussed based on the simulation work.

Keywords: EUV mask, EUV blank, Multi layer, Multi layer defect, Phase defect, Bump, Pit, Inspection. Printability

1 INTRODUCTION

EUV (Extreme Ultraviolet) lithography is one of the most promising techniques for imaging 1x-nm node and below. Other advanced technology may also be used for these nodes, such as NIL (Nano Imprint Lithography), EBDW (Electron Beam Direct Writing) and DSA (Directed Self-Assembly), along with several lithography techniques highlighted today. However, considering process cost and complexity of 1x-nm node and beyond technologies, the leading contender for the next generation lithography is EUV.

There are several challenges associated with EUV lithography from development to HVM, defectivity of masks and blanks are one of the biggest issues that have to be cleared before HVM starts. The structure of EUV blanks is more complicated than that of optical blanks, and it consists of many layers: LTEM (Low Thermal Expansion Material) substrate, backside conductive layer, front side reflective stack of 40 pairs of Mo/Si bilayers, Ru protective capping layer and Ta-based absorber layer. Especially, ML (multilayer) defect is one of the difficult defect types, and the number of multilayer defect needs to be minimized to provide zero printable defect masks from mask maker to wafer fabs. It means EUV blank inspection requires more advanced approaches than the techniques that are employed for optical blanks inspection now. In these years, several inspection tools specific for ML defects have been developed and introduced to the industry. Where both transmitted and reflected light are used for optical mask inspection, only reflected light is available for EUV mask because the masks are reflective.[1,2] But it is very important to consider how sensitivity performance of these tools should be evaluated, and furthermore, it has to be considered how to obtain appropriate test blanks with programmed ML defects. And types and sizes of the programmed ML defects need to be properly characterized. In the past, several evaluation results of programmed ML defects which were fabricated by e-beam writing and etching process have been reported.[3,4] In these reports, normally the

cross-section shape of the programmed defects are rectangle. On the other hand, very curious result are reported that defect printability and defect detectability of rectangular shape programmed defects and natural defects are very different.[4,5] It is considered that such phenomenon could happen because multilayer formation may be different between natural defects and programmed defects due to the shape of defect source as shown in Figure 1. In other word, shape of natural defect is more complicated. It is unlikely happened that cross-section shapes of natural defects are rectangular and top and bottom of natural defects are perfectly flat. From these evaluation results, it is requested to fabricate test blanks with programmed ML defects which show similar characteristics as natural defects. In the past couple of years, we developed new programmed defect fabrication method and showed flexibility to fabricate both rectangle shape defects, which have been fabricated by conventional method, and natural-like programmed defects which represents real situation.[6]

In this paper, it was attempted to fabricate more complex defect shapes and very shallow defects to show a flexibility of the defect fabrication method. Then defect shape characterization work was conducted by AFM to investigate defect shape transition model. Secondly, defect printability was simulated for various defect sizes, and wafer impact caused by size and shape of ML defects was evaluated. Finally, various sizes of defect source were fabricated on substrate based on the simulation result.

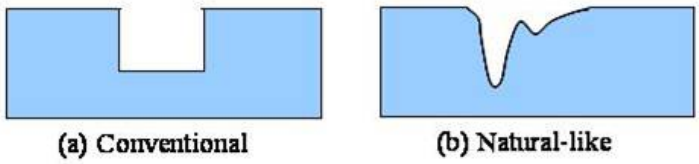

Fig.1 Schematic view of source of programmed defect

2 EXPERIMENTS

2-1 Programmed ML defect blank fabrication

Generally, programmed ML defect blanks have been patterned by e-beam writing and mask process (resist develop, etching and resist strip). Thus, it is easy to fabricate many same height defects by one process cycle, however, number of mask process cycle increases as number of designed defect height increases. On the other hand, our new defect fabrication method has only one process for defect formation, as reported previously.[6] The method enables to fabricate various sizes and shapes of defect source by proper process for required defect types from several processes. After defect fabrication, defect sizes and shapes were measured and characterized by SEM and AFM. Then multilayer was deposited on top of the source of programmed defects under normal deposition conditions using an ion beam deposition tool. Finally defect sizes and shapes after multilayer deposition were measured again and compared with sizes and shapes before multilayer deposition.

2-2 Programmed ML defect types

Figure 2 shows fabricated programmed ML defect samples. One of the defect types we attempted to fabricate is rectangle shape defect. It means, if conventional method is applied for defect formation, programmed defect shape is normally rectangle. So we attempted to reproduce similar defect shape as conventional method fabricates. Other types of programmed defects are suspected to be similar to real substrate defects which are occurred by polishing or cleaning in actual blank fabrication process.

Five different defect types are located in different defect area. Defect sizes were designed from 18x18nm to 1000x1000nm width and wide range of defect height (or depth) from 1nm to 30nm. All dimensions of these programmed defects are on

mask dimensions.

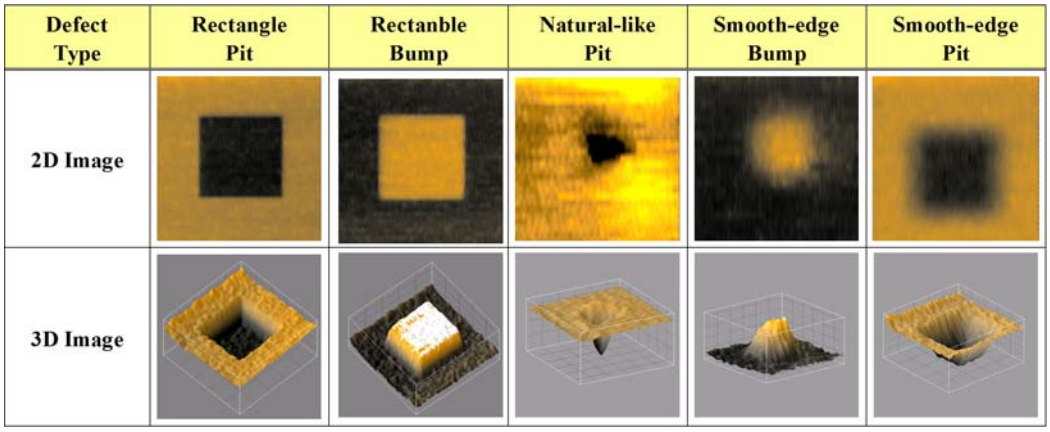

Fig.2 Schematic view of fabricated programmed ML defect sources

3 RESULTS AND DISCUSSION

3-1 Results of more complex defect shape formation

Source of programmed ML defects were fabricated on Qz substrate. There are a couple of concerns that need to be considered. Firstly, the target sizes of the programmed ML defects are relatively smaller than that of regular programmed defects which were historically fabricated for optical mask and it is necessary to measure not only defect width but also defect height or depth. So defect size measurement would be one of the key for programmed defect characterization. Secondly, defect shape on bottom of multilayer and on top of multilayer may be different due to multilayer deposition conditions, and it is very important to understand how the defect shapes transit from the surface of Qz substrate to the top of multilayer. Because difference of ML defect formation models may cause defect printability difference on wafer. So the size of the ML defects needs to be measured before and after multilayer deposition process.

In previous reports, it was confirmed that new defect formation method shows good defect size control in defect depth and width for both rectangle shape defects and natural-like defects.[6,9] According to previous research, ML defect printability depends on shape of defect source and ML decoration model.[7] Generally, small sizes of ML defects have been focused on ML defect printability study, however, it is assumed to be difficult to detect thin and wide defect by blank inspection tool. And also, impact on wafer of this type of defects may be more critical than small defect even if height of the defect is below 1nm in some defect structure model. Based upon the assumption, it was attempted to fabricate very shallow defect sources on substrate by new method. Figure 3 shows defect size measurement result of fabricated very shallow programmed pit defect. The defect sizes were measured by AFM.

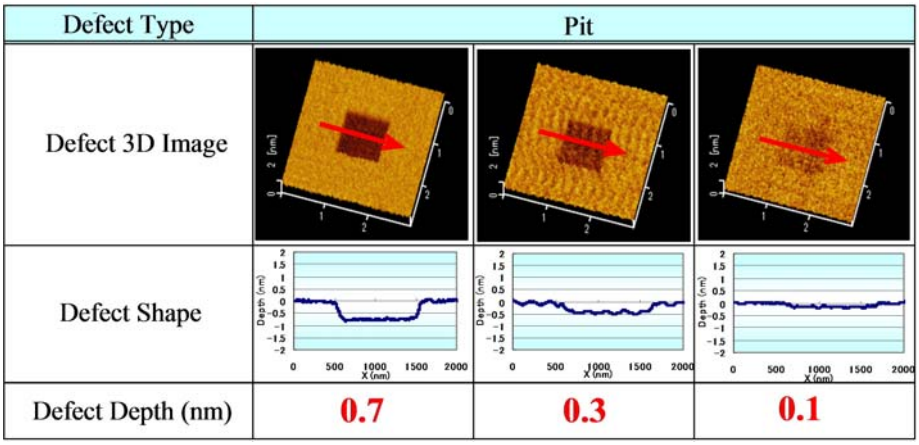

Fig.3 Depth measurement result of shallow programmed defect sources

It was confirmed that target height of half pitch 11nm node (0.7nm) was successfully fabricated.[8] And furthermore, very shallow defect of 0.1nm depth was observed by AFM. From this result, it was verified that the new method shows sufficient performance to fabricate very shallow height defects.

Secondly, it was tested to fabricate more complicated defect shapes to confirm flexibility of the new method. Figure 4 shows the result of fabricated more complicated defect structures on Qz substrate. The result represents that it is very flexible to fabricate arbitrary shapes like multi step defect and smooth-edge defect by application of the new defect fabrication method. Of course, it is suspected whether such complicated shape defects exist in real situation. But the result proves that it is potentially capable to reproduce real defect situation by the new method.

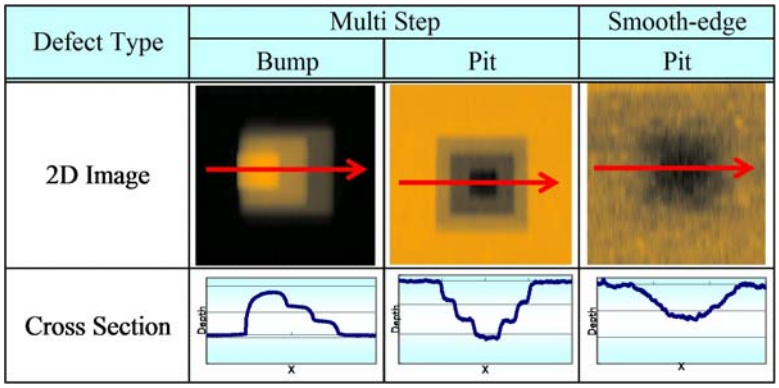

Fig.4 Fabricated complicated structure defect sources

3-2 Defect shape decoration by multilayer deposition

Several types of defect transition model by multilayer deposition have been proposed by many reports. And it is said defect printability on wafer is differ from defect transition model. After defect source fabrication, multilayer deposition work was conducted, and defect shapes were measured before and after multilayer deposition. Figure 5 shows defect shape comparison of fabricated programmed defects.

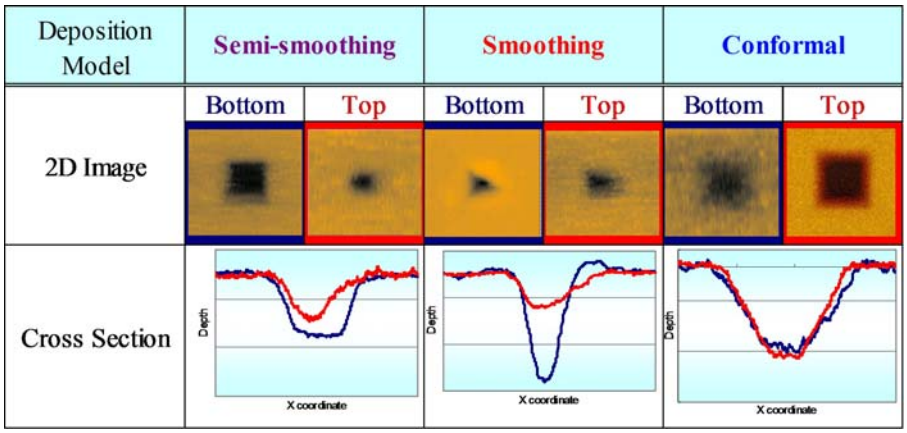

Fig.5 Defect Shape transition between before and after ML deposition

According to the measurement result, actual defect shape transition is very complicated. At least on these 3 defects, 3 different defect transition models, which can be called Smoothing, Semi-smoothing and Conformal, were confirmed. From the result, it seems defect transition model may depend on a slope angle and width of the defects. However, it is very difficult to predict how multilayer defects grow from the bottom to the top of multilayer by seeing just only top shape of the defects. And furthermore, when mask suppliers obtain EUV blanks, the surface of the blanks have been covered with absorber layer, normally. It means, it will be more complicated and difficult to predict real characteristics of the defects through absorber layer.

3-3 Defect Transition Model

Before conducting defect printability simulation, 3 different defect transition models were defined based upon the defect shape measurement result shown in Figure 5. (Figure 6) In the figure, D_{top} and D_{bottom} mean defect depth on surface of ML and bottom of ML.

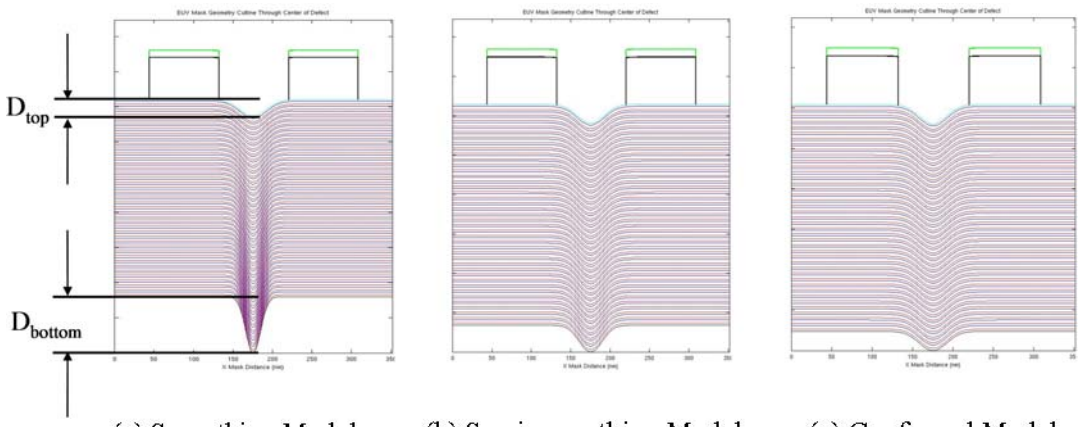

(a) Smoothing Model (b) Semi-smoothing Model (c) Conformal Model

Fig.6 Defect transition models

At first, as for Smoothing model, defect depth on ML surface is reduced 70% from the depth on the bottom of ML. It means $D_{top} = D_{bottom} \times 0.3$. Secondly, regarding Semi-smoothing model, defect depth on ML surface is reduced 30% from the depth on the bottom of ML. It means $D_{top} = D_{bottom} \times 0.7$. At the last, in the conformal model, the defect depth on the surface and the bottom of the multilayer are assumed to be same. So, it means $D_{top} = D_{bottom}$. In any conditions, it was defined that defect volume did not change by ML deposition process. It means defect width is increased due to defect depth reduction. From the actual defect shape measurement result, it seems that the shape of defects may change between before and after ML deposition, however, the definition about the volume and width of ML defects are assumed to be reasonable because ML deposition should be consistent on blank surface regardless of surface topography.

3-4 Defect Printability Simulation

3-4-1 Simulation Condition

On the basis of the defect size measurement result and the defect transition models defined by the measurement results, defect printability simulation was conducted for these 3 models. Defect location relative to the mask absorber pattern is very important for defect printability study. Defect impact on wafer depends on where ML defect locates. It is reported that defect has the biggest impact when the defect location is just center of clear feature, which means the area absorber is stripped off. In this study, half pitch 22nm Line/Space pattern was applied as absorber pattern, and defect location is defined just on the center of clear feature. As a wafer exposure condition, following condition as shown in Table 1 was presumed.

Table 1 Exposure condition for simulation work

Simulation Conditions	
Scale	Mask Scale
Hp	88nm L/S
NA	0.33
Sigma	0.8
Pupil	Conventional
CRA	6degree

3-4-2 Simulation Results

Figure 7 shows the defect printability simulation result by Smoothing model. From the result, narrower defects tend to be printed worse than wider defects even a depth of the defect is shallow.

Figure 8 shows the defect printability simulation result by Semi-Smoothing model. The result looks similar to the result of Smoothing model, however, the impact by Semi-Smoothing model defect shows slightly lower impact than Smoothing model defect.

Figure 9 shows the defect printability simulation result by Conformal model. The result is very close to Semi-Smoothing model.

In these results, it looks very interesting that defect impact on wafer gets smaller as defect width gets wider even if defect depth gets deeper. And also, as smoothing rate gets smaller, the area where defect impact is big, colored in dark or red, gets

smaller.

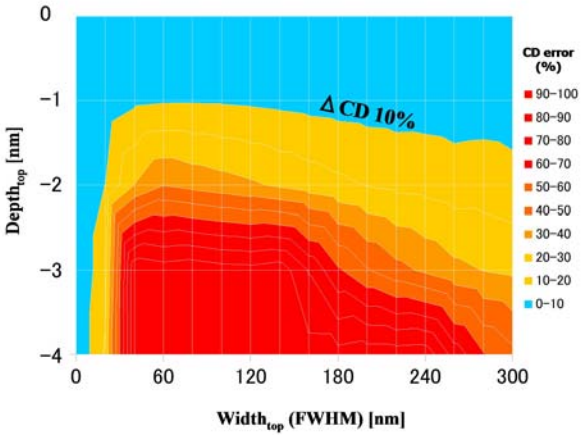

Fig.7 Printability simulation result for Smoothing deposition model

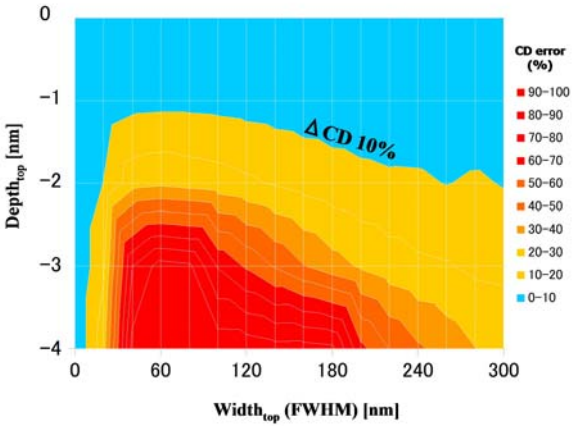

Fig.8 Printability simulation result for Semi-smoothing deposition model

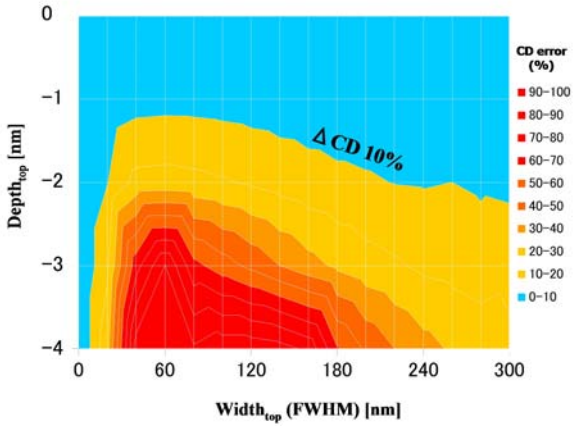

Fig.9 Printability simulation result for Conformal deposition model

ΔCD=10% line was extracted from Figure 7,8 and 9. (Figure 10) From the result, it is clear that 1nm depth and range of 30nm to 150nm width has big impact on wafer regardless of the defect transition model. It is supposed that the point that causes the biggest impact on wafer is just the edge of the defect and it looks very critical how rapidly the defect height or depth changes. It means, EUV light is reflected to wrong direction on the defect edge, and the impact on wafer gets worse.

In this study, it is necessary to investigate whether our new defect source fabrication method is enough capable for programmed defect blanks which are useful for blank inspection qualification. From the point of view of this purpose, the target programmed defect sizes have to include both printable and non-printable defects around ΔCD=10% line which are hatched by yellow in Figure 10. Then it will be possible to fabricate appropriate test blanks with proper defect sizes.

Consequently, it is judged that required defect sizes for the purpose will be width from around 30x30nm to 250x250nm and depth from sub-1nm to 2nm.

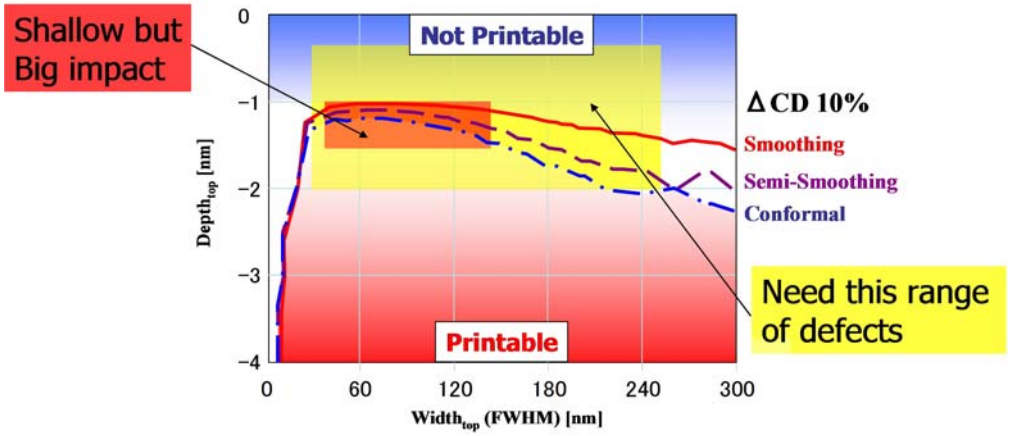

Fig.10 Defect printability comparison among 3 different defect transition models

3-4-3 Target defect fabrication

Based on the printability simulation results, it was attempted to fabricate source of shallow ML defect targeting printable and not-printable defects around marginal print line which described above. Figure 11 shows defect fabrication results for proper size range for programmed defect blanks based upon printability simulation work.

It was confirmed the sizes of the fabricated defect sources were well controlled and succeeded to fabricate target defect sizes for a programmed defect blanks. Whatever the defect transition model is, the defect sizes of the fabricated programmed ML defects after ML deposition will be able to meet the requirement calculated from defect printability simulation.

From these results, the new defect fabrication method is expected to be effective for future ML defect evaluation.

Defect Type	AFM 3D image	Width (FWHM)	Depth
Pit	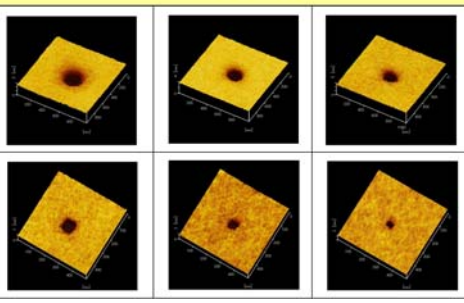	30～250	1.0～2.0

Fig.11 Defect fabrication results for proper size range for programmed defect blanks

4 CONCLUSIONS

In this study, programmed multilayer defect blank has been fabricated and printability of ML defects was simulated for 3 different defect transition models.

Firstly, not only conventional rectangle shape defects but also natural-like defects were successfully fabricated by new

method. It was attempted to fabricate very shallow defects below 1nm depth, and characterization work was conducted by AFM. From the results, it was confirmed that target height of HP 11nm node (0.7nm) was successfully fabricated on substrate. Then it was shown that the new method is very flexible to fabricate very unique defect shape like pyramid and smooth-edge as well. From these results, the new defect fabrication is expected to be capable to reproduce real defect situation.

Secondly, defect shape measurement was conducted before and after multilayer deposition process, and it was confirmed that defect shape transition model is very complicating. Based upon the measurement results, 3 different defect transition models were proposed.

Thirdly, defect printability simulation was conducted to investigate the wafer impact difference among the 3 defect transition models. From the simulation results, it was confirmed that wafer impact is varied by deposition models, but narrower defects tend to be printable even the depth is shallow. And target defect size range for programmed defect blanks was defined as width from around 30x30nm to 250x250nm and height from sub-1nm to 2nm.

Finally, it was attempted to fabricate source of shallow multilayer defects based on the printability simulation results. It was confirmed sizes of the programmed defect sources were well controlled and succeeded to fabricate target size range. And it is expected that the defect size will be appropriate range regardless of whatever defect transition model is.

To conclude, new programmed defect fabrication method showed good effectiveness to provide proper test vehicle which consists of natural-like defects like real situation. And the defect fabrication technique is expected to be useful for future tool evaluation and qualification.

5 ACKNOWLEDGEMENTS

This work was supported by New Energy and Industrial Technology Development Organization (NEDO).
The authors would like to thank the people who contributed to this work.

REFERENCES

1. Takeshi Yamane, Toshihiko Tanaka, Tsuneo Terasawa, Osamu Suga, “Actinic EUVL mask blank inspection capability with time delay integration mode”, Proc. SPIE Vol. 7748, 7748-83 (2010).
2. Joshua Glasser, Stan Stokowski, Gregg Inderhees, “Inspecting EUV mask blanks with a 193-nm system”, Proc. SPIE Vol. 7748, 7748-37 (2010).
3. Pei-Cheng Hsu, et al, “Printability of Buried Mask Defects in Extreme-UV Lithography”, Proc. SPIE Vol. 7969, 7969-47 (2011).
4. Hyuk Joo Kwon, et al, “Printability of Native Blank Defects and Programmed Defects and Their Stack Structures”, Proc. SPIE Vol. 8166, 8166-06 (2011).
5. Takeshi Yamane, Toshihiko Tanaka, Tsuneo Terasawa, Osamu Suga, “Phase defect analysis with actinic full-field EUVL mask blank inspection”, Proc. SPIE Vol. 8166, 8166-05 (2011).
6. Kazuaki Matsui, Noriaki Takagi, Takeshi Isogawa, Yutaka Kodera, Yo Sakata, Shinji Akima, “Novel Programmed Defect Mask Blanks for ML Defect Understanding and Characterization”, Proc. SPIE Vol. 8441, 8441-33 (2012)
7. Takashi Kamo, Tsuneo Terasawa, Takeshi Yamane, Hiroyuki Shigemura, Noriaki Takagi, Tsuyoshi Amano, Kazuo Tawarayama, Mari Nozoe, Toshihiko Tanaka, Osamu Suga and Ichiro Mori, “Evaluation of EUV mask defect using blank inspection, patterned mask inspection, and wafer inspection”, Proc. SPIE Vol.7969, 7969-17 (2011)
8. Kiwamu Takehisa, Hiroki Miyai, Tomohiro Suzuki, Haruhiko Kusunose, Takeshi Yamane, Tsuneo Terasawa, Hidehiro

Watanabe, Soichi Inoue, Ichiro Mori, “EUV Actinic Blank Inspection Tool Development”, EUVL Symposium (2012)
9. Yutaka Kodera, Kazuaki Matsui, Satoshi Takahashi, Yo Sakata, Shinji Akima, “New Test Vehicle with a Variety of Programmed ML Defects for EUV Blanks Inspection”, EUVL Symposium (2012)